



UNIVERSITAT
POLITÈCNICA
DE VALÈNCIA



INSTITUTO DE INGENIERÍA DE
ALIMENTOS PARA EL DESARROLLO

STUDY OF COOKING PROCESS IN HAM BY TERMOGRAPHY AND DIELECTRIC SPECTROSCOPY

MÁSTER EN CIENCIA E INGENIERÍA DE LOS ALIMENTOS
ESPECIALIDAD INGENIERÍA DE PROCESOS Y PRODUCTOS

Alumno: Nuria Balaguer Cuenca

Directores: Pedro J. Fito Suñer

Marta Castro Giráldez

Centro: INSTITUTO UNIVERSITARIO DE CIENCIA E INGENIERÍA DE
ALIMENTOS PARA EL DESARROLLO

STUDY OF COOKING PROCESS IN HAM BY TERMOGRAPHY AND DIELECTRIC SPECTROSCOPY

Balaguer, N.¹, Castro-Giráldez, M.¹, Fito, P.J¹.

RESUMEN

El jamón cocido es uno de los productos cárnicos con mayor nivel de consumo en todo el mundo. Uno de los retos de la industria alimentaria es el desarrollo de métodos analíticos, rápidos, fiables y no destructivos, con el fin de garantizar una alta calidad en este tipo de productos. El objetivo de este estudio fue evaluar la posibilidad de utilizar las propiedades dieléctricas y la termografía infrarroja, como nuevas herramientas para controlar el proceso de cocción en línea. Los análisis efectuados en la región de infrarrojos se realizaron con un cámara térmica PI OPTRIS ® 160 (OPTRIS GmbH, Berlín, Alemania), con un rango espectral de longitud de onda λ de 7,5 a 13 μm . Las emisividades del jamón, registradas por la cámara, se corrigieron utilizando latón y aluminio como materiales de referencia. La evolución de las emisividades corregidas, en función de la temperatura de calentamiento, permitió detectar puntos críticos asociados a las transiciones proteicas que tienen lugar durante el proceso de cocción. Por otro lado, las propiedades dieléctricas se analizaron mediante un sonda coaxial Agilent 85070E conectada a un analizador de redes Agilent E8362B en la gama de frecuencias de 500 MHz a 20 GHz. La evolución de $\Delta T \tan \delta^t$ en función de la temperatura de tratamiento permitió detectar las transiciones de la miosina y el colágeno, que se producen en el transcurso del proceso de cocción. El análisis de las transiciones de fase con la técnica de calorimetría diferencial de barrido (DSC) y un estudio microestructural con Cryo-SEM confirmaron estos resultados.

Palabras clave: Cryo-SEM, DSC, emisividad, infrarrojo, jamón, propiedades dieléctricas, termografía.

RESUM

El pernil olla és un dels productes carnis amb major nivell de consum en tot el món. Un dels reptes de la indústria alimentària és el desenvolupament de mètodes analítics, ràpids, fiables i no destructius, a fi de garantir una alta qualitat en aquest tipus de producte. L'objectiu d'aquest estudi va ser avaluar la possibilitat d'utilitzar les propietats dielèctriques i la termografia infraroja, con noves ferramentes per a controlar el procés de cocción en línea. Les anàlisis efectuats a la regió d'infrarojos es van realitzar amb una cambra

¹ Instituto Univeristario de Ingeniería de Alimentos para el Desarrollo (IU-IAD)
Universidad Politécnica de Valencia. Camino de Vera, s/n 46022. Valencia. España.

termogràfica Optris PI® 160 (Optris GmbH, Berlín, Alemanya), amb un rang espectral de longitud d'ona de 7.5 a 13 μm . Les emissivitats del pernil registrades per la cambra es van corregir utilitzant llautó i alumini, com a materials de referència. L'evolució de les emissivitats corregides, en funció de la temperatura de calfament, va permetre detectar punts crítics associats a les transicions proteiques, que tenen lloc durant el procés de cocció. D'altra banda, les propietats dielèctriques es van analitzar per mitjà d'una sonda coaxial Agilent 85070E connectada a un analitzador de xarxes Agilent E8362B, en la gamma de freqüències de 500 MHz a 20 GHz. L'evolució de $\Delta \text{Tan}\delta^t$, en funció de la temperatura de tractament va permetre detectar les transicions de la miosina i el col.lagen, que es produïxen en el transcurs del procés de cocció. L'anàlisi de les transicions de fase amb la tècnica de Calorimetria Diferencial d'Agranat (DSC) i un estudi microestructural amb Cryo-SEM van confirmar aquests resultats.

Paraules clau: Cryo-SEM, DSC, emissivitat, infraroig, pernil, propietats dielèctriques, termografia.

ABSTRACT

Cooked ham is a well-known product with high consumption levels all over the world. One challenge of food industry is to develop rapid, reliable and non-destructive analytical methods in order to guarantee high quality in this kind of products. The aim of this study was to evaluate the possibility of using dielectric properties and infrared thermography as new tools for controlling the cooking process on-line. Analyses in the infrared region were performed with an Optris PI® 160 thermal imager (Optris GmbH, Berlin, Germany), with a spectral infrared range of wavelength λ from 7.5 to 13 μm . Ham emissivities, registered by camera, were corrected using brass and aluminum as reference materials. Evolution of corrected emissivities, in function of temperature, permitted to detect critical points associated with protein transitions occurred throughout heating treatment. Furthermore, dielectric properties were analyzed by using an Agilent 85070E open-ended coaxial probe connected to an Agilent E8362B Vector Network analyzer, in the frequency range from 500 MHz to 20 GHz. Evolution of $\Delta \text{Tan}\delta^t$, in function of temperature treatment, allowed detecting myosin and collagen transitions. Analysis of phase transitions, with the technique of Differential Scanning Calorimetry (DSC), and a microstructural study with Cryo-SEM confirmed these results.

Key words: Cryo-SEM, dielectric properties, DSC, emissivity, ham, infrared, thermography.

1. INTRODUCTION

Nowadays, the consumer demand of high quality meat products is mainly influenced by several factors such as health concerns, need of convenience or price (Sepulveda *et al.*, 2011; ElMasry *et al.*, 2010). To fulfill consumer's satisfaction it is very important to provide meat products that can better meet market requirements and to refocus the meat industry, on the customer's needs, because it directly impacts on its profitability (Troy and Kerry, 2010). For this reason, meat industry has undergone a considerable development, especially in the field of heat-treated meat products.

Cooked ham is a porcine meat product mainly sold in Europe, with France, Spain and Italy being major consumers. The traditional processing of cooked hams involves the use of brine that can be injected or infused through soaking, followed by the application of heat to form a meat gel. The final quality of the cooked ham depends on several factors but the most important are the origin and composition of the raw hams and the processing conditions (Toldrá *et al.*, 2010).

Cooking of meat products is essential to achieve a palatable and safe product. The meat proteins, approximately 20% of a muscle's weight, represent the main constituents that make up the structure of the meat system. They undergo substantial structural changes on heating and therefore the quality of the meat product, which is mainly governed by the meat structure, also changes drastically after cooking (Tornberg, 2005).

Due to this, knowing the physical properties of the product related to the heating pattern becomes an essential aspect to obtain reliable information on cooking operation. Nevertheless, traditional methods for assessing meat quality attributes are time consuming, destructive and are associated with inconsistency and variability. Implementing on line instrumental techniques, for rapid screening of meat properties, to improve control and classification of the product in mechanized processes are of great interest for both the industry and the consumers (ElMasry *et al.*, 2012). Among these new emerging technologies highlights dielectric spectroscopy and thermal imaging.

Dielectric spectroscopy determines the dielectric properties of a medium as a function of frequency. It is based on the interaction of an electric external field with the sample (Metaxas and Meredith, 1993; Nelson and Datta, 2001); complex permittivity (ϵ_r) (Eq.1) is the dielectric property that describes this interaction (Metaxas and Meredith, 1993; Nelson and Datta, 2001). The real part of complex permittivity is called dielectric constant (ϵ') and the imaginary part is called loss factor (ϵ''). The dielectric constant is related with the capacitance of the material and its ability to store energy, and the dielectric loss factor is related to the absorption and dissipation of the electric field energy in other kinds of energy such as the thermal one.

$$\epsilon_r = \epsilon' - j \cdot \epsilon'' \quad (1)$$

Several studies reveal that changes in physical state affect dielectric properties. Most of the water in muscle is held by capillary action by the

myofibrils. When the muscle is heated, proteins denature, shorten and expel the entrapped juice. Both, actomyosin and collagen denature, causing juice expulsion. The release of water and dissolved ions, mainly calcium and magnesium, into the extracellular spaces should cause a detectable change in the dielectric properties (Hamm, 1966). This is valuable either as a tool to monitor protein denaturation, or important to modeling predictions if the changes are large during heating treatment.

Li and Barringer (1996) monitored changes in the loss factor (ϵ'') of high salt samples at microwave frequencies, and concluded that changes in loss factor corresponded to the denaturation temperature of actomyosin. Bircan and Barringer (2002) monitored variations in dielectric constant (ϵ') and loss factor (ϵ'') from 915 to 2450 MHz in a range of meat, fish and poultry samples from room temperature to 115°C, and found that both dielectric constant (ϵ') and loss factor (ϵ'') suffered an important increase at a temperature which appeared to match the DSC (Differential Scanning Calorimetry) denature temperature of collagen in these foodstuffs. They postulated that this sharp variation could be due to a loss of water and ions from the denatured proteins. Researchers from this group also published a study related to the dielectric properties of two comminuted meat products, pork luncheon roll and white pudding, over the temperature range 5-85°C at both radiofrequency (RF) and microwave (MW) frequencies. Values of loss factor at this range of frequency varied in a significant way ($P < 0.05$). At microwave frequencies, dielectric properties in white pudding tended to peak at 45°C and decrease thereafter, whereas for pork lunch roll, dielectric constant (ϵ') and loss factor (ϵ'') peaked at 65°C which appeared to match potato starch gelatinization within this product (Zhang *et al.*, 2004).

Since the measurement of dielectric properties in this work were taken at intervals of 20°C, and a number of non-meat ingredients were present in the meat product, Brunton *et al.*, (2006) decided to make another similar experiment in order to avoid masking the effect of protein denaturation in dielectric properties. They analyzed the dielectric properties of whole meat across a temperature range of 5-85°C but at 1°C intervals. Results of this study revealed that changes in the dielectric properties of beef muscle across the temperature range employed could be related to the denaturation temperatures for the main structural proteins in meat (especially collagen). They also found that the representation of dielectric properties vs. temperature profiles were markedly different as a function of the frequency analyzed, microwave or radiofrequency respectively.

As mentioned above, apart from the dielectric spectroscopy, a new emerging technique for rapid screening of meat properties to improve heating control is the thermal imaging (TI). TI is a non-destructive, non-contact system of recording temperature by measuring infrared radiation emitted by a body surface (Arora *et al.*, 2008). TI utilizes the radiation emitted to produce a pseudo image of the thermal distribution of a body's surface. In thermography, a large number of point temperatures are measured over an area and processed to form a thermal map or thermogram of the target surface. Thermography with high spatial resolution is a powerful tool for analyzing and visualizing targets with thermal gradients (Gowen *et al.*, 2010).

In the last few years, TI has found applications in biological systems especially in the agriculture sector (Alchanatis *et al.*, 2006; Chaerle *et al.*, 2000; Lamprecht *et al.*, 2002; Stajko *et al.*, 2004; Sugiura *et al.*, 2007; Oerke *et al.*, 2006). Also, it has been employed in various food processing applications including process monitoring, product development and storage analysis. Related to applications in meat products, Ibarra *et al.* (1999) estimated the internal temperature of chicken meat immediately after cooking, using TI working within a spectral range of 3.4-5.0 μm . This study revealed the potential of TI for the real-time determination of the internal temperature of cooked chicken meat in industrial lines to verify that the center of the sample has been achieved the endpoint temperature.

The aim of this work is to develop an on-line control method of the cooking process of ham, through the use of infrared thermography and the dielectric spectroscopy.

2. MATERIALS AND METHODS

2.1 Experimental procedure

Experiments were done using fresh ham collected at 1.5 days postmortem. Semitendinosus, semimembranosus, biceps femoris and quadriceps femoris were separated in order to remove the intermuscular fat. A diagram of the experimental procedure is shown in Figure 1. Dielectric measurements and thermometry analysis were taken in a continuous system. A Differential Scanning Calorimetry (DSC) study was done to analyze the phase transitions in proteins during cooking operation. Finally, changes in the structure of ham due to the heating treatment were analyzed by Low-temperature scanning electron microscopy (Cryo-SEM) in fresh, cooked and mid-cooked samples (Center temperature 50 $^{\circ}\text{C}$).

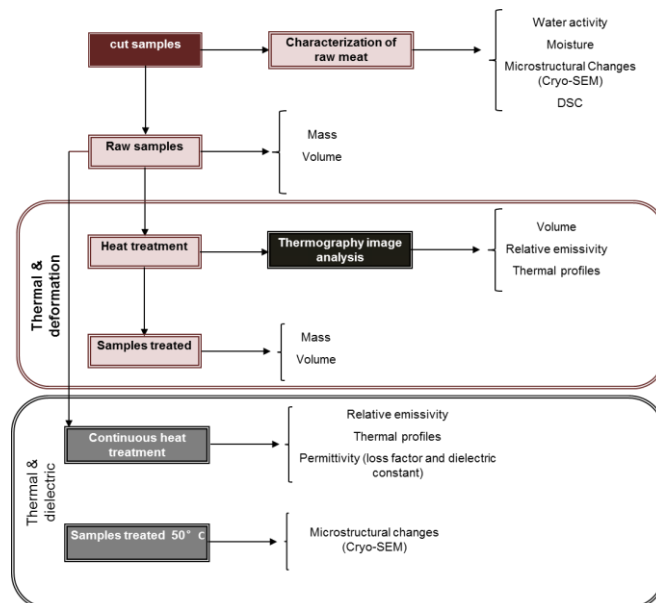


FIGURE 1. Diagram of the experimental procedure.

2.1.1 CONTINUOUS SYSTEM

Cylindrical meat samples of six centimeters of diameter were cooked in a heating jacket connected to a bath equilibrated at 80°C. Real-time cooking operation was performed until the center of the samples reached at a final temperature of 72°C. For the microstructural study, the heating treatment took place until the center of the samples reached at an endpoint temperature of 50 °C, for mid-cooked samples, and 72°C for complete cooked samples. An aluminum strip was placed in the lateral of the heating jacket in order to have a reference emitter for the data registered by the infrared camera. The temperature evolution was controlled by thermocouples placed in the center of the sample and on the sample's surface. Additionally, a third thermocouple was placed in an area between the lateral and the center of the meat samples. Finally, two thermocouple were placed in the lateral of the heating jacket and in the strip of aluminum, respectively, in order to control its temperature. The weight of samples was determined by a precision balance Mettler Toledo AB304-S ($\pm 0,001$), before and after the heating treatment. Changes of volume associated with heating treatment were registered on-line using a visible camera. Subsequently, volume variations were analyzed by image analysis using Adobe photoshop© software. The thermography study and the dielectric properties were recorded on-line. All measurements were taken at 3 min intervals. (See figure 2).

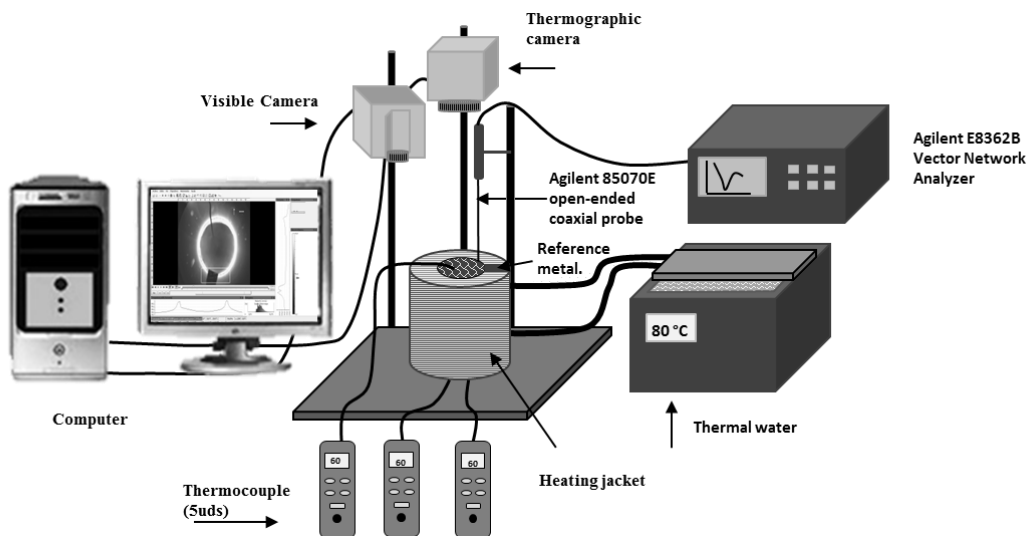


FIGURE 2. Schematic configuration of the continuous system employed for the dielectric measurements and thermography analyses.

2.2. Dielectric properties measurements

The system used to measure dielectric properties consists on an Agilent 85070E open-ended coaxial probe connected to an Agilent E8362B Vector Network Analyzer. The software of the Network Analyzer calculates the dielectric constant and loss factor as a reflected signal function. For these

measurements the probe was fixed to a stainless steel support, and an elevation platform brings the sample near the probe to avoid possible phase changes due to cable movements after calibration. Calibration was performed by using three different types of loads: air, short-circuit and Mili@Q water. All the measurements were registered on-line from 500 MHz to 20 GHz following the direction of fibres.

2.3 Thermography analyses

The thermographic images were recorder with an Optris PI® 160 thermal imager (Optris GmbH, Berlin, Germany), with a spectral infrared range of wavelength λ from 7.5 to 13 μ m, a temperature range of -20 to 100°C and an accuracy of $\pm 2\%$. The detector was a two-dimensional Focal Plane Array that allows a measurement of 160x120 pixels. The camera has a field of view of 23°x17° with a minimal focus distance of 0.02m. The camera is supported by the software Optris PI Connect (Optris GmbH, Berlin, Germany) which offers numerous analysis functions such as point temperatures, temperature profiles, histograms, linescanner function or the determination of the maximum temperature in a defined area. The range of the actual temperature and the standardized colour palettes can be chosen as desire.

2.4 Study of phase transitions: Differential Scanning Calorimetry (DSC)

Thermal transition properties were measured using a DSC 220 CU-SSC5200 (Seiko Instruments) connected to a cooling controller. Samples of around 15-20 mg were enclosed in hermetically sealed aluminium pans (Seiko Instruments, P/N SSC000C008) and then loaded onto the equipment at room temperature. An empty hermetically sealed pan was used as the reference sample. The calibration of the cell was made following the DSC manufacturers' recommendation. Samples were heated from 20°C to 90°C and held at this temperature for 1 min. Heating scans were performed at 10°C/min. The DSC measurements were made by triplicate. Results are presented as average curves. Transition energy (ΔG), expressed as mJ/mg of sample, was calculated from the peak area of the curves.

2.5 Low-temperature scanning electron microscopy (Cryo-SEM)

A CryoA Cryostage CT-1500C unit (Oxford Instruments, Witney, UK), coupled to a Jeol JSM-5410 scanning electron microscope (Jeol, Tokyo, Japan), was used. The sample was immersed in slush N₂ (-210°C) and then quickly transferred to the Cryostage at 1 kPa where sample fracture took place. The sublimation (etching) was carried out at -95°C. The final point was determined by direct observation in the microscope, working at 5 kV. Then, once again in the Cryostage unit, the sample was coated with gold in vacuum (0.2 kPa), applied for 3 min, with an ionization current of 2 mA. The observation in the scanning electron microscope was carried out at 15 kV, at a working distance of 15 mm and a temperature $\leq -130^\circ\text{C}$.

3. RESULTS AND DISCUSSION

3.1 Thermal transition properties of raw ham

The thermal transitions of raw meat samples during heating are shown in figure 3. This figure shows the endotherms corresponding to the consumption of energy required for the breakup of the tertiary and quaternary structure of the major proteins present in meat system and also the formation of a new level of structure. The energy of transition (ΔG) was determined by integrating the area under the curve, taking into account the heating rate and the sample weight (Chiralt *et al.*, 2007). Table 1 lists the values of denaturation temperature and transition energy for each of the sections (a, b and c) shown in Figure 3.

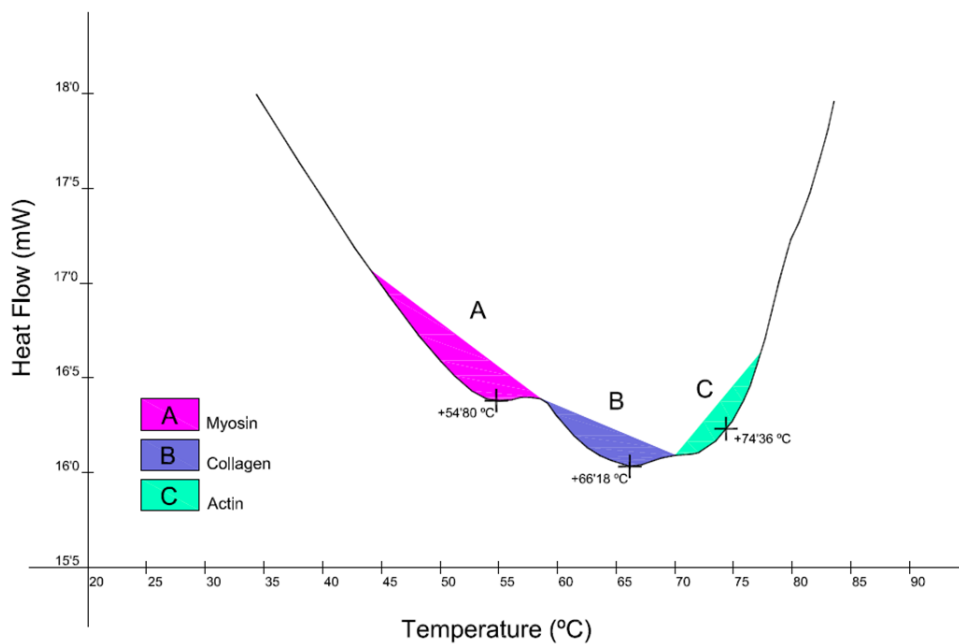


FIGURE 3. Differential scanning calorimetry thermogram of raw ham.

TABLE 1. Parameters of thermal transitions. ΔG : Energy for the thermal transition, T_0 : Initial temperature of transition; T_d : Denaturation temperature; T_f : Final temperature of transition.

Transitions	ΔG (mJ/mg)	T_0 (°C)	T_d (°C)	T_f (°C)
A (Myosin)	0,095	47.4	54.8	56.17
B (Collagen)	0,401	56.87	66.18	67.81
C (Actin)	0,207	68.28	74.36	77.67

Three thermal transitions are visible in the heating flow curve of raw ham with peak values at 54.8, 66.18 and 77.67°C, respectively. Based on the findings of Barbut and Findlay (1991) these peaks most likely are corresponded with denaturation temperatures of myosin (59°C), collagen

(66°C) and actin (82°C), respectively. Previous workers have shown that myosin and actin account for approximately 45% and 25%, respectively, of total myofibrillar protein (Greaser *et al.*, 1981) while collagen is the principle connective tissue protein. It is worth noting the differences in the shapes of the curves. The collagen appeared to have a clear and defined peak while the myofibrillar proteins appeared to have a geometry that makes difficult to obtain the transition energy. A possible explanation could be related with the heating rate employed (10°C/min). Since between the transition temperatures is hardly a difference of 10°C, it could not be enough time for the recovery of the endotherms. Another hypothesis is the overlapping among the transition of proteins and lipids. Kim *et al.*, 2010 documented that the major lipids present in meat have a fusion temperature between 48-60°C. Nevertheless, in our work the lipid content is negligible compared to the protein content. Further work would be needed to investigate these theories.

3.2 Microstructural changes in ham due to heating treatment

Cryo-SEM studies were done in fresh samples, cooked samples and mid-cooked samples. Latter in order to observe the evolution of microstructural changes from the center to the lateral of the samples. The qualitative changes in the microstructure of ham during heating treatment can be appreciated in figure 4. Samples analyzed were studied perpendicular to the directions of fibers.

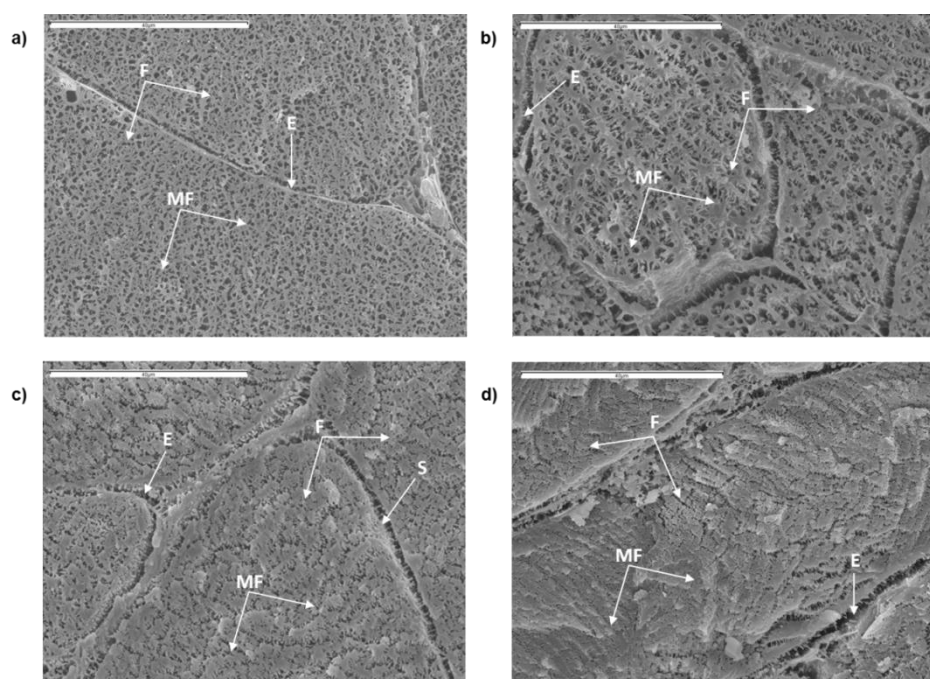


FIGURE 4. Cross-section of *Semimembranosus* muscle of ham observed by Cryo-SEM: raw ham (a), center mid-cooked ham 50°C (b), External region mid-cooked ham 65°C (c), cooked ham 78°C (d). (1500x).e: endomysial connective tissue; f: fibers; mf: myofibrils; s: sarcolemma.

In raw samples (figure 4a) it can be observed a typical dendrite structure produced by the concentration of proteins and water losses due to sublimation that takes place in a Cryo-SEM study (Palka, 1999; Palka and Daun, 1999). As the temperature of cooking increases, notable differences in structural integrity can be noted. Micrograph 4b shows how the cell membranes are relatively damage, as well as the muscle fibers star to experience a transversal and longitudinal shrinkage (Bendall and Restall, 1983; Cheng and Parrish, 1976). These changes can be explained by the progressive denaturation of muscle proteins. Since the micrograph 4b was taken in the center of a mid-cooked sample, the microstructural changes observed could be associated with the denaturation of myosin (See figure 3). In the micrograph 4c, muscle fibers have acquired a granular aspect due to the aggregation and gel formation of sarcoplasmic proteins and the shortening and solubilization of the connective tissue (Bendall and Restall, 1983; Cheng and Parrish, 1976; Palka and Daun, 1999, Rowe, 1989). As in the previous case, this explanation can be confirmed by the temperature of denaturation of connective tissue, registered with the thermogram obtained by DSC (66.18). Finally, micrograph 4c shows how the meat structure has been fully compacted. Since this region of the sample has undergone a greater heating treatment the structural changes previously discussed, have been taken with greater intensity, resulting in a complete loss of structural integrity of meat muscle.

3.2.1 VOLUME VARIATIONS DUE TO HEATING TREATMENT

It should be noted that the changes discussed above include phenomena of expansion and contraction simultaneously. Volume variation experienced by meat pieces, as a consequence of thermal treatment, confirms this behavior. For the calculations of the volume of samples, were considered the mathematical equations that describe the volumes of a cylinder and a skullcap. (See figure 5). Table 2 lists the overall variation of volume in the sample and in the skullcap.

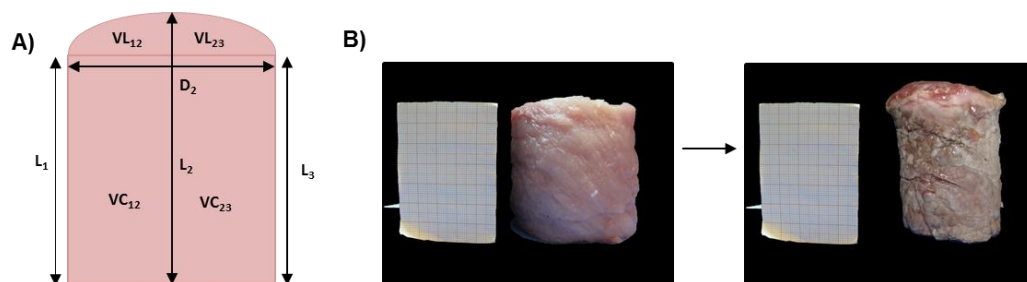


FIGURE 5. a) Schematic diagram of the model used to calculate the volume. Overall volume variation was considered the sum of VL_{12} , VL_{23} , VC_{12} and VC_{23} . b) Example of images analyzed by Adobe photoshop© software.

TABLE 2. Volume variation through the heating treatment.

Time (min)	ΔV (cm ³)		ΔV cap
130	-0,36 ± 0,08	130	0,07 ± 0,02
30	-0,14 ± 0,03	30	0,11 ± 0,04

As shown in Table 2, samples have primarily undergone a shrinking process along the cooking process. However, the phenomena of expansion are reflected in the variation of the volume calculated for the skullcap. The explanation for this trend lies mainly in the behavior of the connective tissue and myofibrillar proteins throughout heating treatment. Denaturation of myosin is associated with expansion phenomena due to the unfolding of the protein chains, which leads to the loss of its tertiary structure. By contrast, the performance of collagen during the cooking process, leads to a tissue contraction. Collagen denaturation probably involves first, the breakage of hydrogen bonds, loosening up the fibrillar structure and then the contraction of the collagen molecule. If unrestrained, collagen fibres, shrink to one-quarter of its resting length on heating to temperatures between 60 and 70°C (Light *et al.*, 1985). If the collagen fibres then are not stabilized by heat-resistant intermolecular bonds, it dissolves and forms gelatin on further heating. Figure 6 shows micrographs where the expansion and contraction process can be qualitatively appreciated.

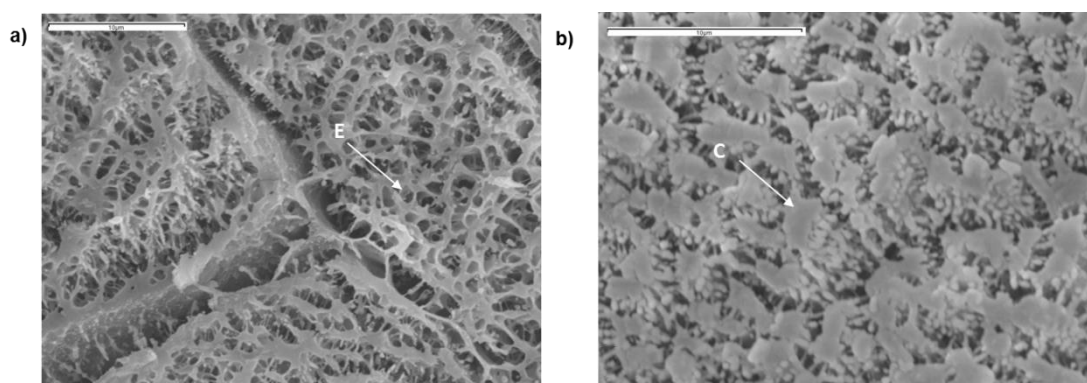


FIGURE 6. Cross-section of *Semimembranosus* muscle of ham observed by Cryo-SEM: a) Expansion of proteic tissue (3500x), b) Contraction phenomena (5000x).

3.3 Analysis by thermal imaging

An infrared thermal imager camera was used in order to measure the heat flux induced in ham and also to determine the evolution of proteins transition fronts. Infrared camera measures the energy received in infrared thermal spectra by a pyrolytic sensor. The basic principle of thermal imaging is based on the fact that, in the temperature range of this work, samples emit in the infrared range (Gowen *et al.*, 2010). Energy emitted depends on the level of the internal energy of the transmitter, Planck developed a law to quantify this relation and Stefan–Boltzmann resumes it as follows (Bulanon *et al.*, 2008):

$$E = \varepsilon\sigma T^4 \quad (2)$$

where E is energy emitted, $W.m^{-2}$, ε is the emissivity of the object, dimensionless, σ is the Stefan–Boltzman constant, $W.m^{-2}.K^{-4}$ and T is absolute temperature, K.

The measurement of this emitted energy can be used to obtain the temperature of the emitting body. The energy measured by the pyrolytic sensor represents the energy emitted by the samples and also the emitted by others materials in the surroundings, thus, other parameters must be consider, like the radiation emitted by the surrounding environment and the transmittance of ambient surrounding, to obtain the real temperature of samples. Due to this, a correction of the temperatures recorded by the camera was done.

3.3.1 CORRECTION OF THE TEMPERATURES RECORDED BY THE THERMOGRAPHIC CAMERA WITH A REFERENCE SYSTEM

Energy absorbed by the pyrolytic sensor represents the overall energy that arrives to the camera, thus, it is possible share out the overall energy in the energy emitted by samples, the absorbed by the air and the reflected by the surroundings of the camera. It is possible to define the overall energy as follows:

$$E = E_s - E_a + E_R = \varepsilon_s\sigma T_s^4 - \sigma(1 - \tau)T_a^4 + \sigma(1 - \varepsilon_R)T_R^4 \quad (3)$$

where, E_s is the energy emitted by meat samples, $W.m^{-2}$, E_a is the energy absorbed by air, $W.m^{-2}$, E_R is the energy from the environment which is reflected, $W.m^{-2}$, ε_s is the emissivity of the meat sample, dimensionless, T_s is absolute temperature of meat sample, K., τ is the transmittance of ambient air, dimensionless, T_a is the temperature of air, K, T_R is the temperature of the surroundings, K, and ε_R is the emissivity of the materials in the surroundings, dimensionless.

Considering that the air transmissivity values are so low and that the distance between the camera and the sample was 20 cm, the second term in Eq. 3 may be considered negligible. Thus, the equation 2 is simplified as follows.

$$E = E_s + E_R = \varepsilon_s\sigma T_s^4 + \sigma(1 - \varepsilon_R)T_R^4 \quad (4)$$

In order to quantify the reflected energy from the surrounding, It has been placed beside the samples on heating jacket, made of brass, a piece of aluminum with emissivity negligible, the two pieces are thermally controlled to determine the difference between the two emitted energy, the result must be the energy reflected by the surroundings.

The average reflected energy obtained by this methodology, throughout the experiments was $152 \pm 12 W/m^2$.

The real energy emitted by meat samples was calculated subtracting the overall energy obtained from the infrared camera, and the reflected energy.

Therefore, the real emissivity of meat was estimated with the temperatures measures by thermocouples and the energy emitted by samples.

Figure 7 shows the evolution of meat emissivity related with the emitted energy of meat samples throughout cooking process, where it is possible to observe how the emissivity evolves with increasing energy emitted, induced by heating (it is produced by the increase of the internal energy, engine of the photon emission).

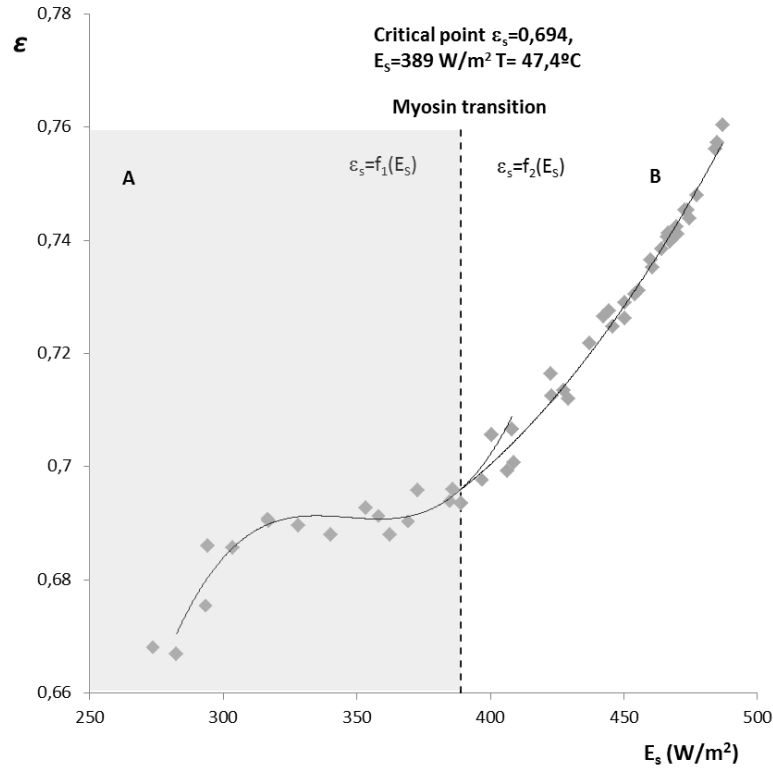


FIGURE 7. Evolution of corrected emissivity with the energy emitted by meat samples.

It can be observed, two different sections, A and B can be distinguished in the evolution of the sample's emissivity with the energy emitted. The first section indicated in figure 7 (A) was adjusted to a polynomial equation of order 3 ($R=0.9612$) while the second adjustment was performed by applying a polynomial equation of order 2 ($R=0.9828$).

Section A includes the beginning of heating till the end of myosin transition, the range temperatures of this transition is comprised between 42.4 and 56 °C (See figure 3), being the half transition temperature 47.4°C.

From the values of corrected emissivity of meat samples it was possible to calculate the temperature profiles and kinetics, as a function of distance and treatment time (Figure 8 and 9 respectively). Temperature profiles were obtained applying Eq.6.

$$T_{S=} = \left(\frac{E_s - E_R}{\sigma E_s} \right)^{1/4} - 273 \quad (6)$$

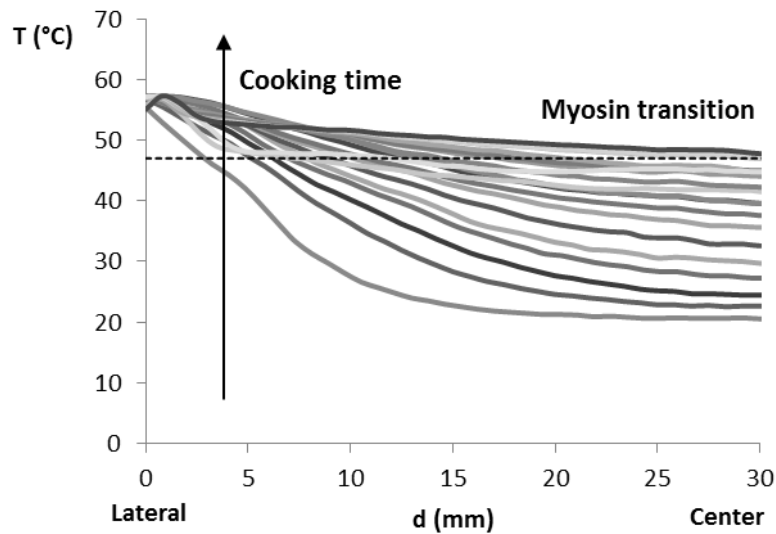


FIGURE 8. Temperature profiles at different times treatment. [Being: 0 min (—), 3 min (—), 6 min (—), 9 min (—), 12 min (—), 15 min (—), 18 min (—), 21 min (—), 24 min (—), 27 min (—), 30 min (—), 33 min (—), 36 min (—), 39 min (—), 42 min (—), 45 min (—), 48 min (—), 51 min (—), 54 min (—)].

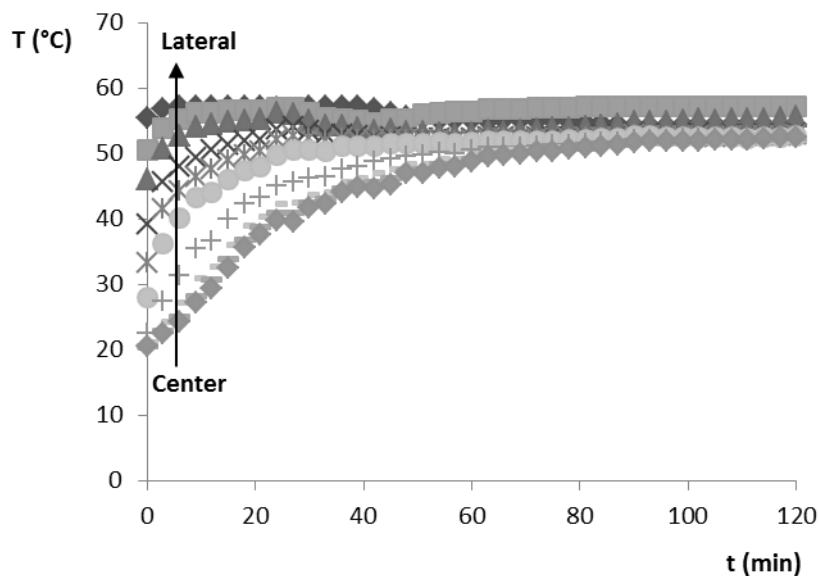


FIGURE 9. Kinetic heating curve at different distances. [Being: 0 mm (◆), 1.62 mm (■), 3.24 mm (▲), 5.68 mm (×), 7.3 mm (✱), 9.73 mm (●), 15.41 mm (+), 20.27 mm (-), 25.14mm (-), 30 mm (◆)].

Figure 8 shows the temperature profiles at different treatment times. Heat flux is share in heating (internal energy), deformations (work) and work flow (latent heat of protein transition), therefore, first times have high energy accumulation, producing a temperature variation near to the lateral, increasing the temperature in the middle slowly. In figure 8, is indicated the threshold where the myosin transition finish. As it can be observed, at the beginning of treatment, this transition is achieved only in the outer areas.

However, at the end of treatment, it can be considered that the myosin transition has taken place in the whole sample.

Figure 9 shows the kinetics of the thermal treatment in different distances from the lateral, of the sample. As occurs in figure 8, as time progresses, in the meat surface, the equilibrium has been reached very fast, a part of this fast accumulation of internal energy is transformed in protein transition (work flow) as the treatment time increases, decreasing the temperature. Figure 10 shows a composition made with images taken with the visible and infrared camera that support these explanations.

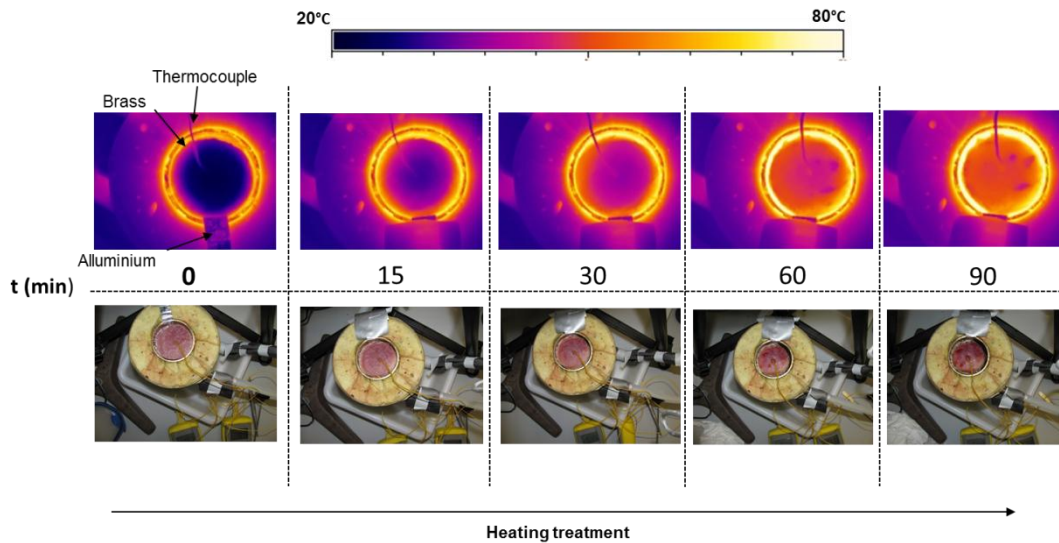


FIGURE 10. Images of the evolution of temperature profiles in meat samples acquired with infrared camera and visible camera.

3.4 Control of heating treatment by dielectric spectroscopy

Dielectric properties were registered on-line in ham samples throughout the heating treatment. Figure 11 shows the dielectric spectra of dielectric constant and loss factor in the microwaves range. At low frequencies, the loss factor shows the effect of ionic conductivity driven by the electric charges of the structure (cations, anions, protein charges, etc). At high frequencies, it is possible to observe in loss factor and in dielectric constant the gamma relaxation, effect related with the orientation and induction of the dipolar molecules. In meat structure the most important dipole is the water molecule, therefore, any interaction between the structure, or with the liquid solutes with the water, must appear in the intensity of signal and in the relaxation frequency of this phenomenon.

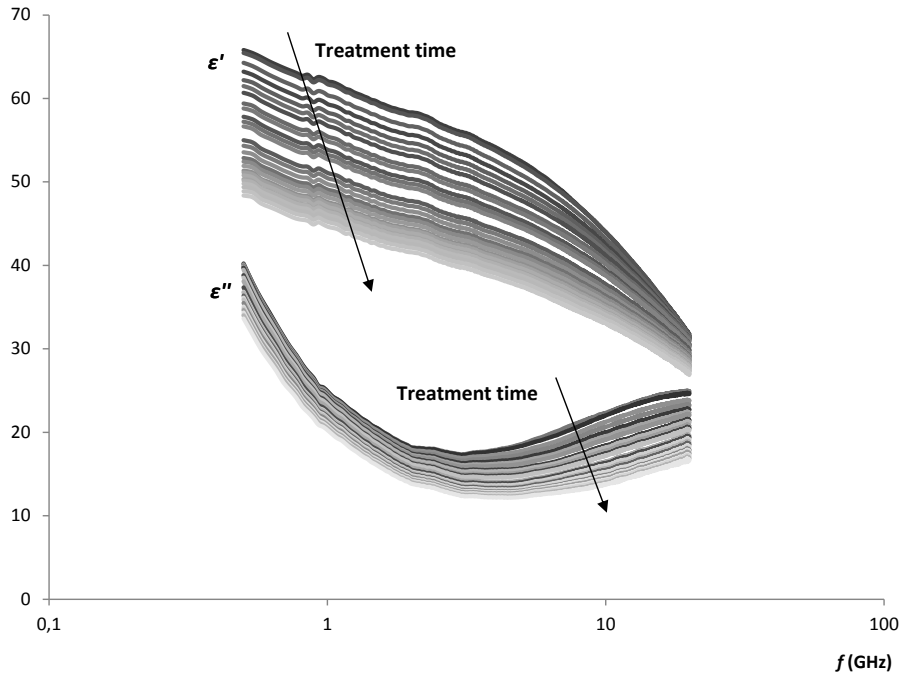


FIGURE 11. Dielectric spectra of ham at different times of treatment.

In Figure 11, it is possible to observe the dependence of the signal with the treatment time, which in turn is intrinsically associated to the accumulation of energy in the structure of meat (internal, latent and mechanical).

The structural changes throughout the heating treatment, explained before, could affect the gamma dispersion and the ionic conductivity. A useful tool to couple both dispersions is the loss tangent. The loss tangent represents the tangent of the permittivity phase (δ) and relates the dissipation with the storage of electric energy. It was calculated as the ratio of the real and imaginary parts of permittivity ($\tan \delta = \epsilon''/\epsilon'$) (Tang, 2005). Figure 12 shows the evolution of loss tangent as a function of time treatment.

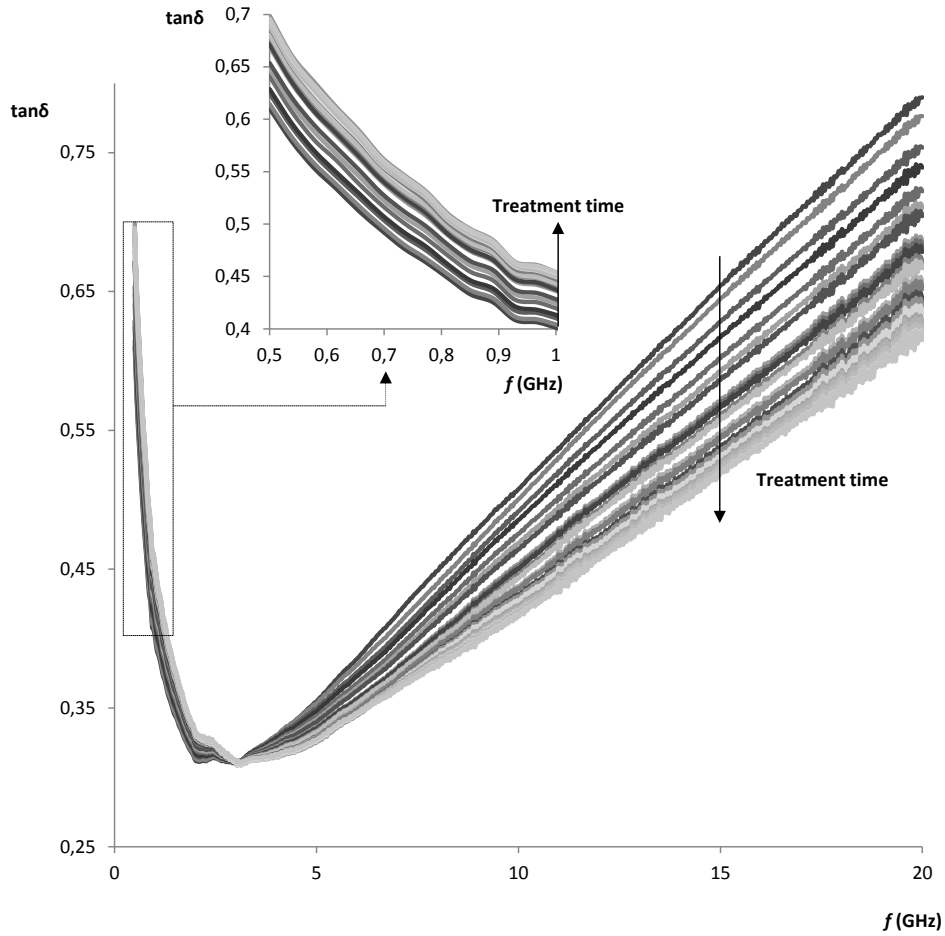


FIGURE 12. Loss tangent ($Tan\delta$) as a function of time treatment.

It can be observed two different tendencies as a function of the frequency analyzed. At low frequencies, the loss tangent tends to increase as the heating treatment enhances, whereas at high frequency the trend observed is the opposite.

In order to obtain clear discrimination of the signal, there were selected two punctual frequencies of 0.5 and 15 GHz to define a parameter related with structural changes occurred in meat samples, (Eq.7).

$$tan\delta_{0.5+15}^t = tan\delta_{0.5\text{ GHz}}^t + tan\delta_{15\text{ GHz}}^t \quad (7)$$

where $tan\delta_{0.5\text{ GHz}}^t$ is the loss tangent at 0.5 GHz on each time cooking, $Tan\delta_{15\text{ GHz}}^t$ is the loss tangent at 15GHz on each time cooking and $Tan\delta_{0.5+15}^0$ is the sum of loss tangent at 0.5 and 15 GHz on time 0.

In order to reduce the effect of the variation of heat flux in the absolute value of permittivity, and also, in the loss tangent, it has been related with the initial value, obtaining the loss tangent increment ($\Delta tg\delta$), as shows next equation, (Eq. 8).

$$\Delta tan\delta^t = \left(\frac{tan\delta_{0.5+15}^t - tan\delta_{0.5+15}^0}{tan\delta_{0.5+15}^0} \right) \quad (8)$$

Figure 13 shows the evolution of $\Delta \tan \delta$ as a function of temperature.

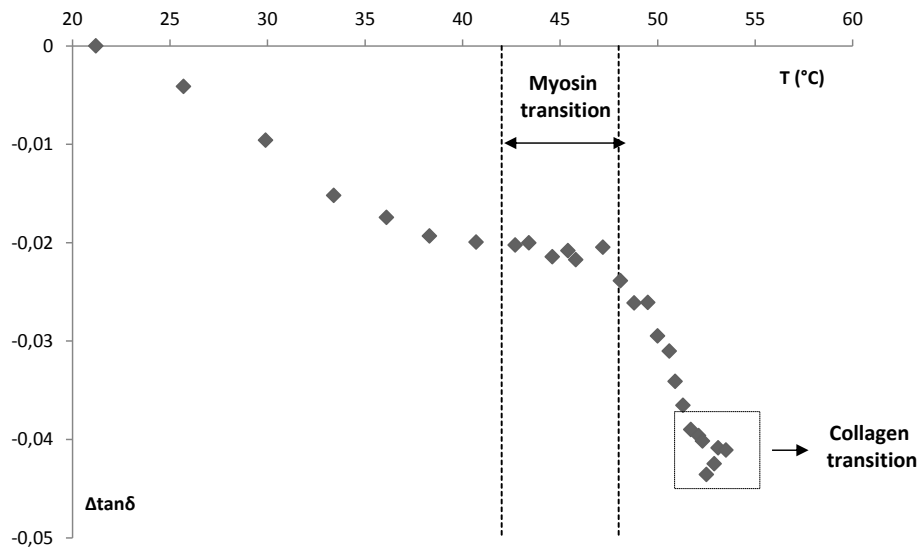


FIGURE 13. Evolution of $\Delta \tan \delta$ as function of heating temperature.

It can be observed three sections clearly differentiated. In the first region, $\Delta \tan \delta$ decreases linearly with increasing temperature. From 42 to 47.4°C $\Delta \tan \delta$ remains constant with a value of $2.08\% \pm 0.07$. This marked change is associated with the transition of myosin as reflected in the thermogram obtained by DSC (See Figure 3). Finally, the last section shows a sharp decrease of the $\Delta \tan \delta$, presenting an accumulation at a temperature of 54°C at the end. This fact can be associated with the transition period of collagen (See Figure 3). At this final point, $\Delta \tan \delta$ acquires a value of $4.13\% \pm 0.15$.

Thus, the accumulation of $\Delta \tan \delta$ in protein transitions shows the possibility to follow online the cooking of ham, allowing the control of the structural changes and therefore, the final quality of the product.

4. CONCLUSIONS

It has been possible to relate the macro and microstructural changes produced in ham, as a consequence of cooking operation, associating those changes to protein and connective tissue transitions.

It has been developed a control method to determine the temperature profiles and the cooking kinetics, by using infrared thermography.

It has been demonstrated that the use of dielectric properties, expressed as variation of loss tangent at different frequencies, are a useful tool to control the cooking process of ham.

5. BIBLIOGRAPHY

Alchanatis, V., Cohen, Y., Cohen, S., Moller, M., Meron, M., Tsipris, J., et al. (2006). Fusion of IR and multispectral images in the visible range for empirical and model based mapping of crop water status. *American Society of Agricultural and Biological Engineers*. Paper no. 061171.

Arora, N., Martins, D., Ruggerio, D., Tousimis, E., Swistel, A. J., Osborne, M. P. (2008). Effectiveness of a noninvasive digital infrared thermal imaging system in the detection of breast cancer. *The American Journal of Surgery*, 196, 523-526.

Barbut, S., Findlay, J. C. (1991). Influence of sodium, potassium and magnesium chloride on thermal properties of beef muscle. *Journal of Food Science*, 56(1), 180-182.

Bendall, J. R., Restall, D. J. (1983). The cooking of single myofibres, small myofibre bundles and muscle strips from beef M. psoas and M. sternomandibularis muscles at varying heating rates and temperatures. *Meat Science*, 8, 93-117.

Bircan, C., Barringer, S. A. (2002). Determination of protein denaturation of muscle foods using the dielectric properties. *Journal of Food Science*, 67(1), 202-205.

Brunton, N. P., Lyng, J. G., Zhang, L., Jacquier, J. C. (2006). The use of dielectric properties and other physical analyses for assessing protein denaturation in beef biceps femoris muscle during cooking from 5 to 85°C. *Meat Science*, 72, 236-244.

Bulanon, D. M., Burks, T. F., Alchanatis, V. (2008). Study on temporal variation in citrus canopy using thermal imaging for citrus fruit detection. *Byosystems Engineering*, 101, 161-171.

Chaerle, L., Van der Straeten, D. (2000). Imaging techniques and the early detection of plant stress. *Trends in Plant Science*, 5(11), 495-501.

Cheng, C. S., Parrish, F. C. Jr., (1976). Scanning electron microscopy of bovine muscle. Effect of heating on ultrastructure. *Journal of Food Science*, 41, 1449.

Chiralt, A., Navarrete, N., Gonzalez, C., Talens, P., Moraga, G. (2007). Propiedades físicas de los alimentos. Ed: Servicio de Publicaciones Universidad Politécnica de Valencia, pp. 57-59.

ElMasry, G., Sun, D.-W. (2010). Meat quality assessment using a hyperspectral imaging system. In: Sun, Da-Wen (Ed.), *Hyperspectral Imaging for Food Quality Analysis and Control*. Academic Press/Elsevier, San Diego, California, USA, pp. 273-294.

ElMasry, G., Sun, D.-W., Allen, P. (2012). Near-infrared hyperspectral imaging for predicting colour, pH and tenderness of fresh beef. *Journal of Food Engineering*, 110, 127-140.

Gowen, A. A., Tiwari, B. K., Cullen, P. J., McDonnell, K., O'Donnell, C. P. (2010). Application of thermal imaging in food quality and safety assessment. *Trends in Food Science and Technology*, 21, 190-200.

Greaser, M. L., Wang, S. M., Lemanski, L. F. (1981). New myofibrillar proteins. *Proceedings of the American Meat Science Association*, 34, 12-16.

Hamm, R. (1966). Heating of muscle systems. In E. J. Briskey, R. G. Cassens, & J. C. Trautman (Eds.). *The physiology and biochemistry of muscle as a food* (p. 363). Madison: University of Wisconsin Press.

Ibarra, J. G., Tao, Y., Walker, J., Griffis, C. (1999). Internal temperature of cooked chicken meat through infrared imaging and time series analysis. *Transactions of ASAE*, 42, 1383-1390.

Kim, B. C., Jeong, D. W., Choi, Y. M., Lee, S. H., Choe, J. H., Hong, K. C., Park, H. C. (2010). Correlations of trained panel sensory values of cooked pork with fatty acid composition, muscle fiber type, and pork quality characteristics in Berkshire pigs. *Meat Science*, 86, 607-615.

Lamprecht, I., Schmolz, E., Blanco, L., Romero, C. M. (2002). Flower ovens: thermal investigations on heat producing plants. *Thermochimica Acta*, 391(1-2), 107-118.

Li, A., Barringer, S. (1996). Effects of protein denaturation on the dielectric properties for ham, egg and milk. *IFT Annual Meeting Book of Abstracts*, 60-2, 141.

Light, N., Champion, A. E., Voyle, C., Bailey, A. J. (1985). The role of epimysial, perimysial and endomysial collagen in determining texture in six bovine muscles. *Meat Science*, 13, 137-149

- Metaxas, A.C., Meredith, R.J., 1993. Industrial Microwave Heating. In: IEE Power Engineering Series 4, Peter Peregrinus LTD, London, UK.
- Nelson, S.O., Datta, A.K., 2001. Dielectric properties of food materials and electric field interactions. In: Datta, A.K., Anantheswaran, R.C. (Eds.), Handbook of Microwave Technology for Food Applications. Marcel Dekker, New York, pp. 69- 114.
- Oerke, E. C., Steiner, U., Dehne, H. W., Lindenthal, M. (2006). Thermal imaging of cucumber leaves affected by downy mildew and environmental conditions. *Journal of Experimental Botany*, 57(9), 2121-2132.
- Palka, K. (1999). Changes in intramuscular connective tissue and collagen solubility of bovine M. semitendinosus during retorting. *Meat Science*, 53, 189–194.
- Palka, K., Daun, H. (1999). Changes in texture, cooking losses, and myofibrillar structure of bovine M. semitendinosus during heating. *Meat Science*, 51, 237–243.
- Rowe, R. W. D. (1989). Electron microscopy of bovine muscles: II – The effects of heat denaturation on post rigor sarcolem and endomysium. *Meat Science*, 26, 281–294.
- Sepulveda, W.S., Maza, M.T., Pardos, L. (2011). Aspects of quality related to the consumption and production of lamb meat consumers versus producers. *Meat Science*, 87, 366–372.
- Stajniko, D., Lakota, M., Hocevar, M. (2004). Estimation of number and diameter of apple fruits in an orchard during the growing season by thermal imaging. *Computers and Electronics in Agriculture*, 42(1), 31-42.
- Sugiura, R., Noguchi, N., Ishii, K. (2007). Correction of low-altitude thermal images applied to estimating soil water status. *Biosystems Engineering*, 96(3), 301-313.
- Tang, J. (2005). Dielectric properties of foods. In: Microwave processing of Foods. (Ed.) H. Schubert. Cambridge, GBR: Woodhead Publishing, Ltd., pp. 22-33.
- Toldrá, F., Mora, L., Flores, M. (2010). Cooked ham. In F. Toldrá (Ed.), Handbook of meat processing New York: John Wiley and Sons, pp. 301–311.
- Tornberg, E. (2005). Effects of heat on meat proteins-Implications on structure and quality of meat products. *Meat Science*, 70, 493-508.
- Troy, D.J., Kerry, J.P., 2010. Consumer perception and the role of science in the meat industry. *Meat Science*, 86, 214-226.
- Zhang, L., Lyng, J. G., Brunton, N. P. (2004). Thermal and dielectric properties of meat batters over a temperature range of 5–85 °C. *Meat Science*, 68, 173–184.